CHAPTER

6 Fluorescent proteins for quantitative microscopy: Important properties and practical evaluation

Nathan Christopher Shaner
The Scintillon Institute, San Diego, California, USA

CHAPTER OUTLINE

Abstract

More than 20 years after their discovery, fluorescent proteins (FPs) continue to be the subject of massive engineering efforts yielding continued improvements. Among these efforts are many aspects that should be of great interest to quantitative imaging users. With new variants frequently introduced into the research community, "tried and true" FPs that have been relied on for many years may now be due for upgrades to more modern variants. However, the dizzying array of FPs now available can make the initial act of narrowing down the potential choices an intimidating prospect. This chapter describes the FP properties that most strongly

Methods in Cell Biology, Volume 123, ISSN 0091-679X, http://dx.doi.org/10.1016/B978-0-12-420138-5.00006-9

impact their performance in quantitative imaging experiments, along with their physical origins as they are currently understood. A workflow for evaluating a given FP in the researcher's chosen experimental system (e.g., a specific cell line) is described.

6.1 OPTICAL AND PHYSICAL PROPERTIES IMPORTANT FOR QUANTITATIVE IMAGING

The breadth of properties in currently available FP variants (Chudakov, Matz, Lukyanov, & Lukyanov, 2010; Shaner, Patterson, & Davidson, 2007) is frequently a source of confusion and frustration among researchers simply wishing to choose the best FP for their particular experiment. Unfortunately, the default position is often to fall back to old FP constructs that are unlikely to provide optimal performance, especially for quantitative fluorescence experiments. At the same time, evaluation of all possible FPs in each experimental context is highly impractical given the huge number of options. The following section enumerates several of the most important properties to consider when narrowing down candidates for use in quantitative microscopy. A listing of the physical and optical properties of some of the most favorable FP choices for quantitative fluorescence imaging is shown in Table 6.1, along with comments on specific advantages and disadvantages of particular variants.

6.1.1 COLOR AND BRIGHTNESS

Foremost among the properties usually noted for FPs are color (excitation and emission wavelength) and brightness (determined by extinction coefficient and quantum yield). Both of these can significantly impact quantitative imaging performance.

The FP color should be chosen carefully to avoid interference from cellular autofluorescence. In general, for mammalian cells, autofluorescent emission is primarily confined to the blue to yellow region of the spectrum, with excitation up to about 500 nm (Aubin, 1979). Thus, for mammalian systems, FPs with longer excitation and emission wavelengths will increase contrast with autofluorescent background. In other systems with a greater number of photoactive components, the situation is more complicated. In plant cells, it is often the shorter-wavelength FPs such as blue emitters that are the most favorably placed relative to autofluorescence (and in some cases, red-orange emitters) (Roshchina, 2012). In any case, it is important to evaluate control (nonexpressing) cells for the intensity and wavelength distribution of autofluorescence prior to performing quantitative image analysis. Brightness of the FP variant used for a quantitative experiment also comes into play in this analysis, since the brighter the FP, the greater the contrast will be, relative to any autofluorescence that is present in a given cell type.

As with most imaging experiments, brighter FPs, provided that their other properties are favorable, are usually preferable choices. Luckily, very bright FPs across most of the visual spectrum are now available, though those at the red end of the

Table 6.1 Optical and physical properties of selected FPs useful in quantitative imaging

Protein name[a]	λ_{ex}[b]	λ_{em}[c]	ε[d]	Φ[e]	Photostability (wide-field)[f]	Comments
mTurquoise2[g]	434	474	30,000	0.93	90	Highest QY true cyan monomer
mTFP1[h]	462	488	64,000	0.85	110	Single-peak "teal" monomer
mEGFP[i]	488	507	56,000	0.60	150	Monomeric variant of EGFP
mEmerald[j]	487	509	57,000	0.68	101[k]	Fast initial bleaching component
mWasabi[l]	493	509	70,000	0.80	93	Brightest "green" monomer
mNeonGreen[m]	506	517	116,000	0.80	158	Brightest monomer
Clover[n]	505	515	111,000	0.76	50	Weak dimer
mVenus[o]	515	528	92,000	0.57	15	Faster maturation, more acid-sensitive
mCitrine[p]	516	529	77,000	0.76	49	Brightest YFP variant
mOrange2[q]	549	565	58,000	0.60	228	Slow maturation
TagRFP-T[q]	555	584	81,000	0.41	337	Most photostable monomer
mRuby2[n]	559	600	113,000	0.38	123	Brightest red monomer
mCherry[r]	587	610	72,000	0.22	96	Simple photobleaching curve
mKate2[s]	588	633	62,500	0.40	118	Brightest long-wavelength

[a] *All proteins shown in this table are monomeric unless otherwise noted.*
[b] *Major excitation peak (nm).*
[c] *Major emission peak (nm).*
[d] *Extinction coefficient (M^{-1} cm^{-1}).*
[e] *Fluorescence quantum yield.*
[f] *Time to reach half of initial fluorescence output at a wide-field illumination intensity giving an initial fluorescence output of 1000 photons per second per chromophore (Shaner, Steinbach, & Tsien, 2005).*
[g] *Goedhart et al. (2012).*
[h] *Ai, Henderson, Remington, and Campbell (2006).*
[i] *Shaner et al. (2007)* and *Zacharias, Violin, Newton, and Tsien (2002).*
[j] *Cubitt, Woollenweber, and Heim (1999)* and *Zacharias et al. (2002).*
[k] *Measured in cells as H2B fusion; due to fast initial bleaching component, the photostability of Emerald variants is difficult to measure precisely (Shaner et al., 2005, 2007).*
[l] *Ai, Olenych, Wong, Davidson, and Campbell (2008).*
[m] *Shaner et al. (2013).*
[n] *Lam et al. (2012).*
[o] *Nagai et al. (2002)* and *Zacharias et al. (2002).*
[p] *Griesbeck, Baird, Campbell, Zacharias, and Tsien (2001)* and *Zacharias et al. (2002).*
[q] *Shaner et al. (2008).*
[r] *Shaner et al. (2004).*
[s] *Shcherbo et al. (2009).*

spectrum have still not caught up to the brightest green and yellow variants. Brightness is largely determined by the inherent optical properties of the folded FP (quantum yield and extinction coefficient) but can also be heavily influenced by the folding efficiency of a given FP variant in a particular cell line. Most modern FPs fold quickly and efficiently in most systems, but it is still important to consider this as a potential factor when comparing FPs for use in a specific experiment. Several comprehensive reviews of FPs have been published over the years, many of which provide in-depth information about various aspects of FP engineering and expression (among many helpful reviews, Chudakov et al., 2010; Miyawaki, 2011; Shaner et al., 2005, 2007; Tsien, 1998; Wachter, Watkins, & Kim, 2010).

6.1.2 PHOTOSTABILITY

Photostability is among the most critical parameters to consider when choosing FPs for quantitative imaging experiments. Even the most photostable FP variants do undergo some degree of photobleaching during the course of most experiments, and so even when choosing high-stability variants, it is important to understand and correct for this behavior in order to obtain quantitative image data. Because FP behavior may be altered depending on localization (e.g., photobleaching may be faster when localized to oxidative organelles such as the ER), culture conditions, or specific illumination source and intensity used for a particular experiment, it is essential to measure this behavior in the specific context planned for a given experiment. In Section 6.4, we describe a workflow for determining the photobleaching curve for specific FP fusions in your system of choice.

6.1.3 OTHER PROPERTIES

Several other properties come into play when choosing an FP variant for quantitative imaging. Among these are ion and pH sensitivity (Griesbeck et al., 2001), tendency to dimerize or form higher-order oligomers (Campbell et al., 2002; Yarbrough, Wachter, Kallio, Matz, & Remington, 2001; Zacharias et al., 2002), folding efficiency (Nagai et al., 2002), and tendency to disrupt the localization or behavior of fusion partners. Ion sensitivity is no longer a common problem in modern FP variants, since they are commonly screened for this behavior during the engineering process. When selecting an FP to target to acidic compartments or to a subcellular environment whose pH may not be stable, one must take into account the fluorescence p*K*a of the FP to ensure that its output will not be impacted by this environment. Generally, cyan, green, and yellow FPs tend to be more pH-sensitive than red FPs, but there is wide variation in this property among available variants.

For the majority of applications, truly monomeric fluorescent proteins are the best choice as a fusion tag, since they are the least likely to cause aberrant behavior or localization of their fusion partner. Unfortunately, many FP variants that have been

previously described as "monomeric" continue to display a small tendency to dimerize under conditions of high local concentration. Only more recently have functional tests such as the OSER assay (Costantini, Fossati, Francolini, & Snapp, 2012) been employed to evaluate the "monomericness" of FPs inside mammalian cells (Shaner et al., 2013), and so for older FPs, such data may not be available. Likewise, the standard of testing many different fusions to a novel FP variant for its initial publication is fairly new, and systematic data on fusion tag performance are sorely lacking for many older or less commonly used FPs. Thus, it is important to carefully evaluate a given FP variant for signs of interference with native function and localization of its fusion partner.

6.2 PHYSICAL BASIS FOR FLUORESCENT PROTEIN PROPERTIES

In the many years since they were first discovered, our knowledge of the complex posttranslational chemistry that takes place in FPs has steadily accumulated. The origins of many important FP optical and physical properties are now well understood.

6.2.1 DETERMINANTS OF WAVELENGTH

All naturally occurring FPs share the same general three-dimensional structure and the same core p-hydroxybenzylidene-imidazolinone chromophore structure, which is formed autocatalytically from the peptide backbone by cyclization and oxidation of an X-Tyr-Gly tripeptide. This basic chromophore absorbs either near-UV (~400 nm) or blue (~488 nm) depending on the protonation state of the phenolate moiety and emits green (~510 nm) (Tsien, 1998). Modifications to this chromophore structure that increase or reduce the number of conjugated double bonds lead to red- and blue-shifted excitation and emission spectra, respectively (Miyawaki, Shcherbakova, & Verkhusha, 2012; Shu, Shaner, Yarbrough, Tsien, & Remington, 2006; Tsien, 1998). Other factors, such as charge interactions or pi-orbital stacking, have significant (but usually smaller) impacts on excitation and emission wavelength.

The first synthetic modifications to the core chromophore structures were substitutions of the central tyrosine for other aromatic amino acids, producing cyan (Tyr → Trp) and blue (Tyr → His) variants of GFP (Tsien, 1998). The chromophore within DsRed, the first of many red-emitting FPs to be discovered (Matz et al., 1999), is extended by two additional double bonds through an additional oxidation of the main peptide backbone, producing an acylimine moiety (Gross, Baird, Hoffman, Baldridge, & Tsien, 2000; Yarbrough et al., 2001). Since these two types of chromophore variant were discovered, many other variations have been identified in naturally occurring FPs or engineered through rational design, producing FPs that span practically the entire visible spectrum in emission wavelengths (Ai, Shaner, Cheng, Tsien, & Campbell, 2007; Shaner et al., 2004; Shcherbo et al., 2009).

6.2.2 DETERMINANTS OF BRIGHTNESS

The brightness of an FP is determined by how effectively its chromophore absorbs incoming light and how efficiently this absorbed energy is converted back into emitted fluorescence. These two factors are known as extinction coefficient and quantum yield.

The peak molar extinction coefficient is related to the absorbance cross section of the FP chromophore and essentially describes how strongly the chromophore absorbs light at its peak absorbance wavelength. Extinction coefficient in FPs can be viewed in two different ways, both of which are useful when evaluating an FP for practicality. The *absolute extinction coefficient* is an intrinsic property of the chromophore, while the *effective extinction coefficient* is additionally influenced by folding and maturation efficiency of the FP.

First, one may consider the absolute extinction coefficient of a properly folded FP molecule with a mature chromophore, at its peak absorbance wavelength. This is the parameter reported in the primary literature for FPs, because it is very easy to measure and does not vary between systems (e.g., the measured value will be the same in protein purified from *E. coli* or in mammalian cells). The absolute extinction coefficient is usually measured by comparing absorbance spectra of the FP before and after denaturation by sodium hydroxide, which unfolds the protein and converts most chromophores into a "universal" form with a known extinction coefficient (Chalfie & Kain, 2006). This value is a best-case scenario for FP performance, because it does not take into consideration the folding efficiency of the FP.

The second way to view FP extinction coefficient is the effective extinction coefficient of the entire population of expressed FP (either alone or as a fusion to another protein). In this case, the protein concentration is determined through a quantitative means (such as absorbance at 280 nm or Bradford assay). This effective extinction coefficient is always lower than the absolute extinction coefficient because no population of FP molecules will exhibit 100% folding and maturation efficiency in any system. This parameter may, in fact, differ very greatly between expression systems and thus can be a major determinant of the practicality of a particular FP in a specific experiment. Unfortunately, because its value is generally idiosyncratic to the specific expression system and fusion partner, it is necessary to determine it empirically for each new experiment, and quantitative data are scarce on how effective extinction coefficient varies between systems for different FPs.

Beyond the simplified "peak extinction coefficient," it may also be useful to consider the peak shape and area under the curve for absorbance spectra of individual FP variants. In general, FPs with relatively narrow absorbance peaks have higher extinction coefficients, while FPs with broader absorbance peaks have lower extinction coefficients. However, differences in extinction coefficient cannot be entirely explained by peak shape. While for most practical purposes it is possible to compensate for differences in peak shape or even in absolute extinction coefficient, by adjusting illumination intensity and/or using different filter sets, in some cases, peak shape becomes important and must be taken into account when designing an experiment (particularly when using multiple labels, to minimize overlap in excitation). Figure 6.1 illustrates the diversity of absorbance peak shapes and extinction coefficients among FPs.

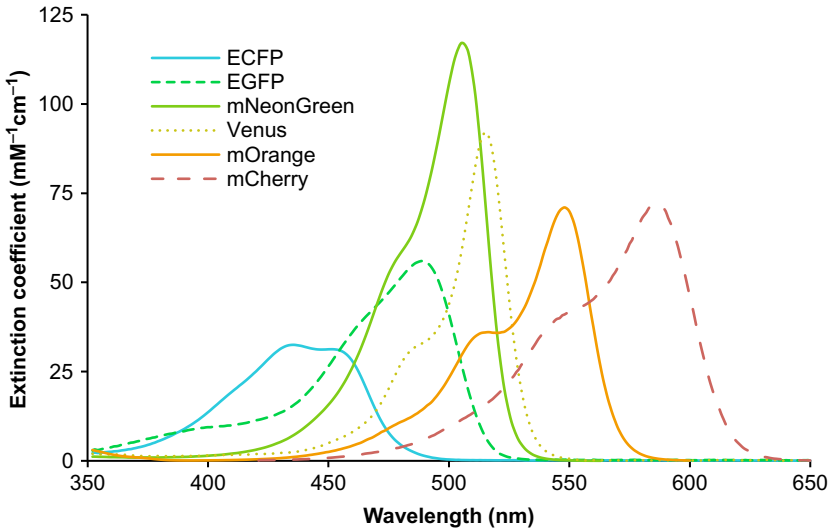

FIGURE 6.1

Absorbance spectra of the representative FPs ECFP (Cubitt et al., 1999), EGFP (Tsien, 1998), mNeonGreen (Shaner et al., 2013), Venus (Nagai et al., 2002), mOrange (Shaner et al., 2004), and mCherry (Shaner et al., 2004), in order from lowest to highest absorbance peak wavelength. Absolute absorbance curves for each FP are scaled to their peak extinction coefficients, illustrating the wide variations in peak shape and area under the curve (AUC) for various FPs. Among the FPs shown, mNeonGreen displays the largest AUC (100%), followed by mCherry (95%), EGFP (73%), mOrange (72%), Venus (66%), and ECFP (45%).

The quantum yield of a particular FP, unlike the effective extinction coefficient, rarely varies between expression systems. Quantum yield is simply the fraction of absorbed photons that lead to emitted fluorescence. When a chromophore absorbs an incoming photon, it enters an excited state that can typically return to the ground state via several parallel mechanisms, one of which is emission of a photon (fluorescence). The fraction of excited state chromophores returning to the ground state via the emissive pathway is the quantum yield. Other pathways for relaxation to the ground state involve energy transfer to other parts of the protein (as heat), and so FPs with fewer options for nonemissive relaxation have higher quantum yields. One of the major determinants of this is the planarity of the chromophore, with more planar chromophores generally displaying higher quantum yields (Shu et al., 2006).

6.3 THE COMPLEXITIES OF PHOTOSTABILITY

Photostability is among the most important FP properties to consider when choosing a variant for quantitative imaging. Fluorescent proteins are frequently described as "highly photostable" or "poorly photostable," but this superficial

description says very little about this potentially very complex behavior. Described in the succeeding text are several important factors to consider when evaluating the photostability of a given fluorescent protein.

6.3.1 MULTIPLE PHOTOBLEACHING PATHWAYS

Photobleaching in fluorescent proteins is rarely observed as a single-exponential decay of emitted fluorescence. This is primarily due to the presence of multiple pathways capable of deactivating the fluorescence (either permanently or transiently) of the chromophore. Known and theorized pathways for photobleaching include (1) *cis* to *trans* isomerization of the double bond adjacent to the chromophore phenolate, (2) photochemical decarboxylation of glutamate or aspartate side chains in the vicinity of the chromophore, (3) oxidative modification of side chains proximal to the chromophore, (4) oxidative modification of the chromophore itself, (5) temporary but long-lived chromophore protonation, (6) other photochemical reactions leading to cleavage or modification of the chromophore, and (7) entry of the excited state chromophore into a triplet state via a "forbidden" singlet-to-triplet transition, followed by relaxation to the ground state with a long half-life (Chalfie & Kain, 2006; Chapagain, Regmi, & Castillo, 2011; Dean et al., 2011; Duan et al., 2013; McAnaney et al., 2005; Regmi, Bhandari, Gerstman, & Chapagain, 2013; Shaner et al., 2008; Sinnecker, Voigt, Hellwig, & Schaefer, 2005). Some of these processes (2, 3, 4, and 6) may lead to permanent bleaching or other permanent changes in the optical characteristics of the FP. Others (1, 5, and 7) are generally reversible and/or temporary. This mix of potential bleaching pathways begets the complex bleaching curves observed for most FPs.

Controllable reversible conversion to a dark state (often termed "photoswitching") is a highly useful property for specialized applications such as single-molecule superresolution microscopy (Patterson, Davidson, Manley, & Lippincott-Schwartz, 2010). However, for the purposes of this discussion, we will exclude photoswitchable and photoconvertible FP variants and focus instead on "traditional" FPs with simpler photobleaching decay curves.

6.3.2 PHOTOBLEACHING BEHAVIORS

Most fluorescent proteins display at least two major photobleaching components, each with a different half-time of roughly exponential decay. These components (both their magnitude and half-times) are individual to each fluorescent protein variant and have been fully characterized for very few variants to date. To complicate matters, one or both of these major components may be partly or fully reversible, meaning that if not left under constant illumination, some portion of the fluorescence will recover in the dark with its own half-time (which may additionally be temperature dependent, among other things) (Shaner et al., 2008; Sinnecker et al., 2005). Many fluorescent proteins also display some degree of photoactivation upon

illumination, which may temporarily increase their fluorescence emission until the entire population of chromophores has been activated and bleaching becomes dominant. One or more photobleaching or photoactivation components may also be oxygen-dependent (Regmi et al., 2013; Shaner et al., 2008).

Some examples of complex photobleaching curves for common fluorescent proteins are shown in Fig. 6.2, illustrating the different behaviors observed depending on the dominant components of photobleaching. Of particular note are the large differences in behavior observed between continuous illumination (the standard method of measuring photostability) and intermittent illumination (the standard method of performing real-world imaging experiments) (Fig. 6.3), which can be partially explained by the phenomenon of reversible dimming (Fig. 6.4).

The simplest expectation of photobleaching is that the rate of a given component will scale linearly with the illumination intensity (or equivalently, the initial light output of the FP population). Indeed, photobleaching rates are usually roughly linearly proportional to illumination intensity within ~1 order of magnitude of the intensity used for measurement. However, when illumination intensity is much higher or lower than that used for measurement, photobleaching behavior is frequently very different. This may be due in part to rate-limiting factors such as oxygen diffusion that favor nonoxidative photobleaching pathways

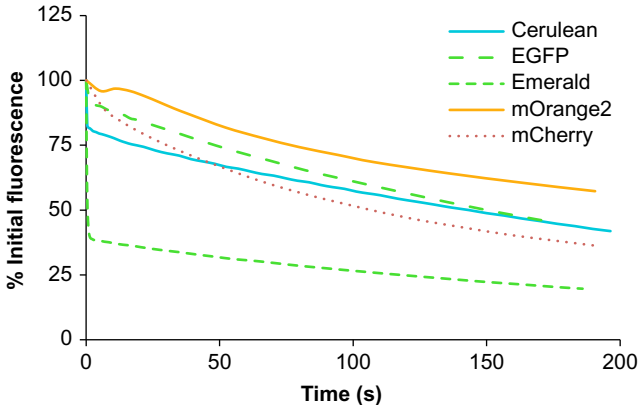

FIGURE 6.2

Wide-field photobleaching curves of the representative FPs Cerulean (Markwardt et al., 2011), EGFP (Tsien, 1998), Emerald (Tsien, 1998), mOrange2 (Shaner et al., 2008), and mCherry (Shaner et al., 2004). Several types of multicomponent fluorescence decay curves are illustrated from these examples, including fast early bleaching (Emerald and Cerulean) and photoactivation (mOrange2). Both EGFP and mCherry have simpler curves than many other FPs. The timescale is adjusted such that each curve represents an initial output of 1000 photons per second per chromophore under continuous illumination (Shaner et al., 2005).

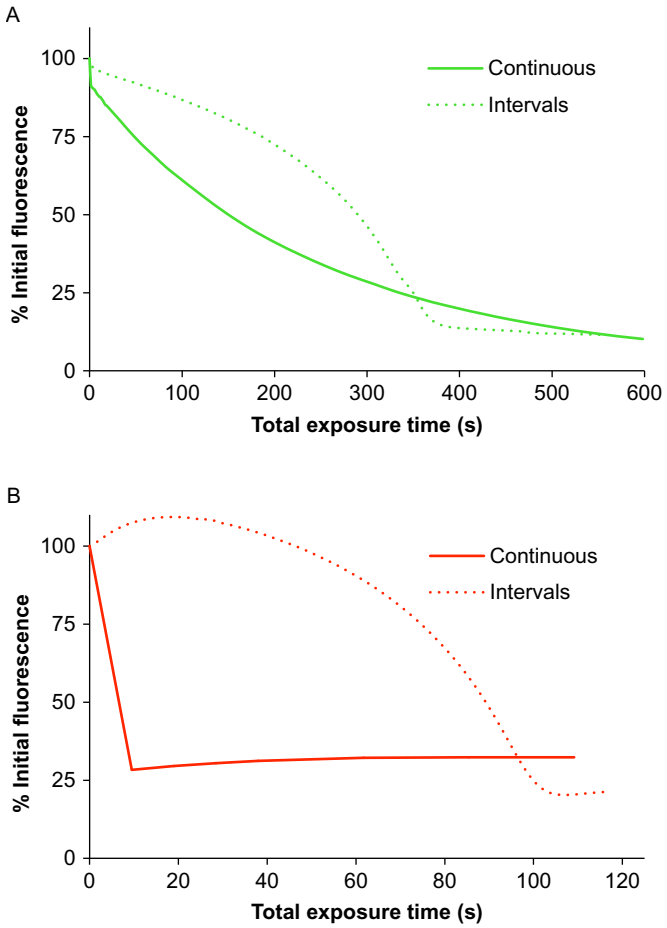

FIGURE 6.3

Photobleaching behavior differs depending on exposure regimen. Two notable examples are shown here: (A) EGFP (Tsien, 1998) displays markedly nonexponential fluorescence decay when imaged intermittently, compared to an almost-exponential decay curve under continuous illumination; (B) mApple (Shaner et al., 2008) displays a very fast initial bleaching component followed by a prolonged plateau under continuous illumination but appears far more photostable (but highly nonexponential) when imaged intermittently. The timescale is adjusted such that each curve represents an initial output of 1000 photons per second per chromophore. Intermittent illumination curves were obtained using a 200-ms exposure every 10 s; the timescale for intermittent illumination represents the cumulative exposure time (i.e., not counting the periods between exposures).

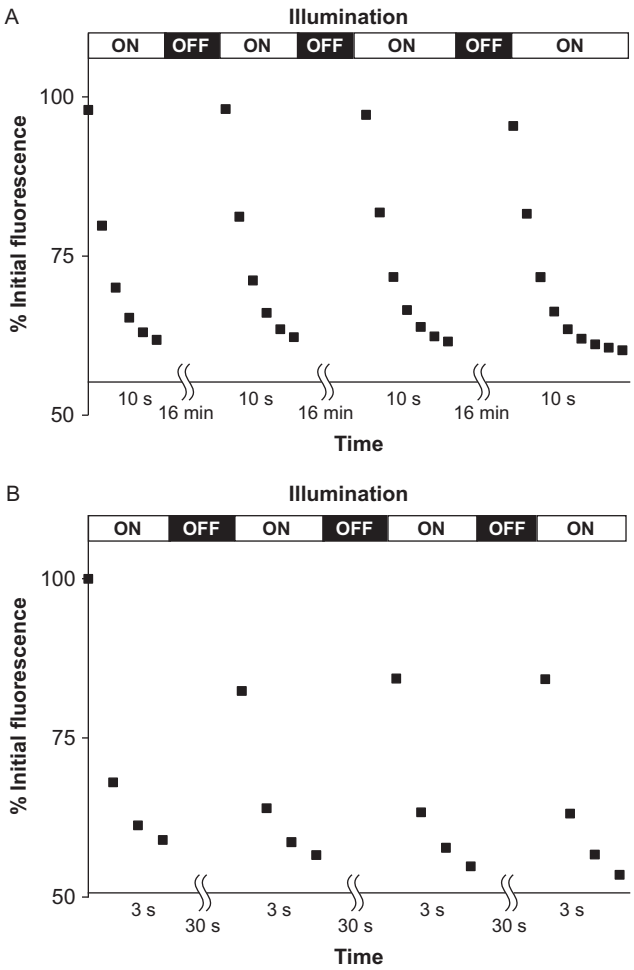

FIGURE 6.4

Reversible dimming in FPs. Many commonly used FPs display a behavior similar to photochromism in which they reversibly lose fluorescence under continuous illumination. Among the many examples, (A) Cerulean (Rizzo, Springer, Granada, & Piston, 2004) loses ~40% of its initial fluorescence upon continuous exposure to high-intensity wide-field illumination for 10 s but recovers nearly all of this emission brightness if left in the dark for approximately 16 min (Shaner et al., 2008); (B) mApple (Shaner et al., 2008) displays even faster kinetics for reversible dimming, losing nearly half of its initial brightness within ~3 s and regaining 80% or more after only 30 s in the dark. Whether this process is similar to photoswitching in other FPs (such as Dronpa; Ando, Mizuno, & Miyawaki, 2004) remains unclear.

under very high illumination intensities (Duan et al., 2013). As a result, the relative photostabilities of different FPs measured using wide-field arc-lamp illumination typically bear little relation to those observed for laser-scanning confocal illumination.

Due to these many complexities, it is critical to evaluate photostability of an FP in as close to the same illumination regime as will be used experimentally, taking into account the intensity, duration, and interval of illumination in order to determine which bleaching behaviors will contribute to changes in fluorescence over the course of an experiment. By carefully measuring these effects, it is possible to correct for even the most complex FP photobleaching behaviors.

6.3.3 REPORTING STANDARDS FOR FP PHOTOSTABILITY

Unfortunately, despite years of discussion among the scientific community, there remains no set standard for measuring and reporting FP photostability in the literature. Since most photobleaching behavior is nonexponential and contains multiple components with different time constants, expressing FP photostability as a single-exponential time constant is not very meaningful. Increasingly, journals expect authors to provide full photobleaching curves for novel FPs, which is helpful only if these curves are measured in a way that allows for direct comparison to other FPs. It is this author's opinion that the most reliable way to compare FP photostabilities is to (1) measure them in living cells, (2) normalize to a standard of known half-time (EGFP, e.g., loses 50% of its initial fluorescence in 150 s under an illumination intensity that produces 1000 emitted photons per second per chromophore; Shaner et al., 2007), and (3) verify all photobleaching behaviors under a variety of illumination intensities and intervals. Until a universally accepted standard for literature reporting of FP photostability materializes (an unlikely possibility), researchers would be well advised to rely primarily on their own real-world comparisons of FP performance, as described in the next section.

6.4 EVALUATION OF FLUORESCENT PROTEIN PERFORMANCE *IN VIVO*

Among the most critical prerequisites for performing quantitative fluorescence microscopy is a thorough understanding of the behavior of one's chosen fluorescent protein probe(s) in the system of interest. While the basic physical and optical characterization data presented in most primary fluorescent protein literature provide a broad view of the performance of individual variants, there are too many potentially complicating factors to predict with high confidence whether a given variant will perform well in a specific experiment. Because of this unfortunate reality, the best approach is generally to evaluate each potential FP tag in a context as similar as possible to the intended experiment. Among the factors that should be considered are (1) cell type; (2) culture conditions; (3) cameras, microscope optics, and filter sets;

(4) illumination intensity; (5) exposure duration and frequency; and (6) subcellular environment experienced by the FP fusion.

6.4.1 CELL-LINE-SPECIFIC PHOTOSTABILITY AND CONTRAST EVALUATION

Several factors can improve the quality of data collected to evaluate the performance of one or many fluorescent proteins in a given cell line of interest. Confining the FP to a subcellular compartment such as the nucleus generally produces much less cell-to-cell variation than expression of an unfused FP that will be present mainly in the cytoplasm. Analysis can be simplified further by fusion of the FP to a relatively non-diffusible protein such as histone 2B (H2B) (Shaner et al., 2007). Fusion to H2B holds the additional advantage of allowing the observation of mitosis in the target cell line, in order to determine whether the FP interferes with the function of its fusion partner.

This evaluation workflow allows for the comparison of fluorescent proteins of any wavelength class for practicality in a given imaging setup and cell type. To rank FPs for their usefulness in a given quantitative imaging experiment, it is most important to consider (1) the contrast of FP fluorescence versus cellular autofluorescence and (2) the FP's general photostability and photobleaching decay curve under experimental conditions. In theory, it is possible to correct for both of these effects if careful measurements are taken using the appropriate controls.

PROTOCOL

1. Construct expression plasmids encoding H2B fusions to each FP (both N- and C-terminal fusions of H2B behave similarly, but both can be tested if desired).
2. Transfect cultured cells in No. 1.5 coverslip bottom dishes with H2B fusions and incubate 24–48 h under normal culture conditions; keep several nontransfected controls under identical growth conditions.
3. For each FP, choose filter sets appropriate to the excitation and emission spectra. If no specific filter set is described in the primary literature on the FP, consult filter manufacturers, who frequently have online tools for comparing spectra and recommending filter sets. If all else fails, contact the author of the primary publication for advice on choosing the best filter set.
4. Conduct imaging using the same microscope, objective, filter set, temperature, and atmosphere intended for later experiments. Ensure that all microscope components and culture dishes have equilibrated to the experimental temperature and atmosphere prior to commencing imaging.
5. Adjust neutral density filters to achieve the lowest illumination intensity possible while scanning the culture dish for a suitable field of cells to image—this minimizes "prebleaching" that will confound analysis later.
6. Once a suitable field of cells for imaging has been identified and the microscope focused, immediately discontinue illumination for at least 5 min prior to commencing photobleaching experiments—this will allow most reversible dimming to recover prior to measurement. If focus drifts significantly

during the waiting period, this generally indicates that one or more components (microscope objective, culture dish, etc.) have not yet equilibrated to temperature.

7. Image cells using exposure times, illumination intensity, and interexposure intervals similar to those planned for the intended experiments. It may be useful to perform a range of exposure regimens to cover the most likely range of intensities, on times, and off intervals to be used later. Ensure that at least 10–20 cells are imaged for each regimen in one or multiple fields.
8. Analyze intensity data for as many cells as possible in the field of view for each run. Large variances in measured photobleaching curves may indicate nonuniformity in illumination over the field of view. Average photobleaching curves for each illumination regimen can then be used as calibration standards to correct for photobleaching in experimental data obtained under identical regimens.
9. Image nontransfected cells using identical illumination and exposure settings to those used for transfected cells for several frames; this will provide a basis for determining FP contrast with autofluorescence, which may also photobleach over time.

6.4.2 FUSION PROTEIN-SPECIFIC FP EVALUATION

Once the list of FP candidates for a given experiment has been narrowed down, it can be highly useful to perform additional evaluation of each FP in a context more similar to the ultimate experimental system. Several factors are important to note, including whether the FP perturbs localization or function of the fusion partner and whether the specific subcellular milieu of the fusion partner affects the fluorescence or photostability of the FP. This evaluation should follow the general workflow of the previous section, using the fusion(s) in question under well-controlled conditions. To verify correct localization of FP fusions, it can be helpful to use immunofluorescence staining in transfected and identical nontransfected cells as a reference.

CONCLUSION

Careful evaluation of FPs is a critical step prior to gathering important data in quantitative fluorescence microscopy experiments. Several factors influence the performance of a given FP in each experimental system, and no single FP can be classified as the “best choice” for all experiments. By following the guidelines described here, it is possible to determine which among the ever more numerous FP variants are most likely to perform well in a given context and to produce useful data to correct for photobleaching artifacts and autofluorescence. This workflow can be further extended to determine more complex photobleaching behavior in multilabeling and FRET experiments.

REFERENCES

Ai, H.-W., Henderson, J. N., Remington, S. J., & Campbell, R. E. (2006). Directed evolution of a monomeric, bright and photostable version of Clavularia cyan fluorescent protein: Structural characterization and applications in fluorescence imaging. *Biochemical Journal*, *400*(3), 531–540. http://dx.doi.org/10.1042/BJ20060874.

Ai, H.-W., Olenych, S. G., Wong, P., Davidson, M. W., & Campbell, R. E. (2008). Hue-shifted monomeric variants of Clavularia cyan fluorescent protein: Identification of the molecular determinants of color and applications in fluorescence imaging. *BMC Biology*, *6*, 13. http://dx.doi.org/10.1186/1741-7007-6-13.

Ai, H.-W., Shaner, N. C., Cheng, Z., Tsien, R. Y., & Campbell, R. E. (2007). Exploration of new chromophore structures leads to the identification of improved blue fluorescent proteins. *Biochemistry*, *46*(20), 5904–5910. http://dx.doi.org/10.1021/bi700199g.

Ando, R., Mizuno, H., & Miyawaki, A. (2004). Regulated fast nucleocytoplasmic shuttling observed by reversible protein highlighting. *Science*, *306*(5700), 1370–1373. http://dx.doi.org/10.1126/science.1102506.

Aubin, J. E. (1979). Autofluorescence of viable cultured mammalian cells. *Journal of Histochemistry and Cytochemistry: Official Journal of the Histochemistry Society*, *27*(1), 36–43.

Campbell, R. E., Tour, O., Palmer, A. E., Steinbach, P. A., Baird, G. S., Zacharias, D. A., et al. (2002). A monomeric red fluorescent protein. *Proceedings of the National Academy of Sciences of the United States of America*, *99*(12), 7877–7882. http://dx.doi.org/10.1073/pnas.082243699.

Chalfie, M., & Kain, S. R. (2006). *Green fluorescent protein: Properties, applications, and protocols*. Hoboken, NJ: Wiley-Interscience.

Chapagain, P. P., Regmi, C. K., & Castillo, W. (2011). Fluorescent protein barrel fluctuations and oxygen diffusion pathways in mCherry. *Journal of Chemical Physics*, *135*(23), 235101. http://dx.doi.org/10.1063/1.3660197.

Chudakov, D. M., Matz, M. V., Lukyanov, S., & Lukyanov, K. A. (2010). Fluorescent proteins and their applications in imaging living cells and tissues. *Physiological Reviews*, *90*(3), 1103–1163. http://dx.doi.org/10.1152/physrev.00038.2009.

Costantini, L. M., Fossati, M., Francolini, M., & Snapp, E. L. (2012). Assessing the tendency of fluorescent proteins to oligomerize under physiologic conditions. *Traffic (Copenhagen, Denmark)*, *13*(5), 643–649. http://dx.doi.org/10.1111/j.1600-0854.2012.01336.x.

Cubitt, A. B., Woollenweber, L. A., & Heim, R. (1999). Understanding structure-function relationships in the Aequorea victoria green fluorescent protein. *Methods in Cell Biology*, *58*, 19–30.

Dean, K. M., Lubbeck, J. L., Binder, J. K., Schwall, L. R., Jimenez, R., & Palmer, A. E. (2011). Analysis of red-fluorescent proteins provides insight into dark-state conversion and photodegradation. *Biophysical Journal*, *101*(4), 961–969. http://dx.doi.org/10.1016/j.bpj.2011.06.055.

Duan, C., Adam, V., Byrdin, M., Ridard, J., Kieffer-Jaquinod, S., Morlot, C., et al. (2013). Structural evidence for a two-regime photobleaching mechanism in a reversibly switchable fluorescent protein. *Journal of the American Chemical Society*, *135*(42), 15841–15850. http://dx.doi.org/10.1021/ja406860e.

Goedhart, J., von Stetten, D., Noirclerc-Savoye, M., Lelimousin, M., Joosen, L., Hink, M. A., et al. (2012). Structure-guided evolution of cyan fluorescent proteins towards a quantum yield of 93%. *Nature Communications*, *3*, 751. http://dx.doi.org/10.1038/ncomms1738.

Griesbeck, O., Baird, G. S., Campbell, R. E., Zacharias, D. A., & Tsien, R. Y. (2001). Reducing the environmental sensitivity of yellow fluorescent protein. Mechanism and applications. *Journal of Biological Chemistry*, *276*(31), 29188–29194. http://dx.doi.org/10.1074/jbc.M102815200.

Gross, L. A., Baird, G. S., Hoffman, R. C., Baldridge, K. K., & Tsien, R. Y. (2000). The structure of the chromophore within DsRed, a red fluorescent protein from coral. *Proceedings of the National Academy of Sciences of the United States of America*, *97*(22), 11990–11995. http://dx.doi.org/10.1073/pnas.97.22.11990.

Lam, A. J., St-Pierre, F., Gong, Y., Marshall, J. D., Cranfill, P. J., Baird, M. A., et al. (2012). Improving FRET dynamic range with bright green and red fluorescent proteins. *Nature Methods*, *9*(10), 1005–1012. http://dx.doi.org/10.1038/nmeth.2171.

Markwardt, M. L., Kremers, G.-J., Kraft, C. A., Ray, K., Cranfill, P. J. C., Wilson, K. A., et al. (2011). An improved cerulean fluorescent protein with enhanced brightness and reduced reversible photoswitching. *PLoS One*, *6*(3), e17896.

Matz, M. V., Fradkov, A. F., Labas, Y. A., Savitsky, A. P., Zaraisky, A. G., Markelov, M. L., et al. (1999). Fluorescent proteins from nonbioluminescent Anthozoa species. *Nature Biotechnology*, *17*(10), 969–973. http://dx.doi.org/10.1038/13657.

McAnaney, T. B., Zeng, W., Doe, C. F. E., Bhanji, N., Wakelin, S., Pearson, D. S., et al. (2005). Protonation, photobleaching, and photoactivation of yellow fluorescent protein (YFP 10C): A unifying mechanism. *Biochemistry*, *44*(14), 5510–5524. http://dx.doi.org/10.1021/bi047581f.

Miyawaki, A. (2011). Development of probes for cellular functions using fluorescent proteins and fluorescence resonance energy transfer. *Annual Review of Biochemistry*, *80*, 357–373. http://dx.doi.org/10.1146/annurev-biochem-072909-094736.

Miyawaki, A., Shcherbakova, D. M., & Verkhusha, V. V. (2012). Red fluorescent proteins: Chromophore formation and cellular applications. *Current Opinion in Structural Biology*. http://dx.doi.org/10.1016/j.sbi.2012.09.002.

Nagai, T., Ibata, K., Park, E. S., Kubota, M., Mikoshiba, K., & Miyawaki, A. (2002). A variant of yellow fluorescent protein with fast and efficient maturation for cell-biological applications. *Nature Biotechnology*, *20*(1), 87–90. http://dx.doi.org/10.1038/nbt0102-87.

Patterson, G., Davidson, M., Manley, S., & Lippincott-Schwartz, J. (2010). Superresolution imaging using single-molecule localization. *Annual Review of Physical Chemistry*, *61*, 345–367. http://dx.doi.org/10.1146/annurev.physchem.012809.103444.

Regmi, C. K., Bhandari, Y. R., Gerstman, B. S., & Chapagain, P. P. (2013). Exploring the diffusion of molecular oxygen in the red fluorescent protein mCherry using explicit oxygen molecular dynamics simulations. *Journal of Physical Chemistry B*, *117*(8), 2247–2253. http://dx.doi.org/10.1021/jp308366y.

Rizzo, M. A., Springer, G. H., Granada, B., & Piston, D. W. (2004). An improved cyan fluorescent protein variant useful for FRET. *Nature Biotechnology*, *22*(4), 445–449. http://dx.doi.org/10.1038/nbt945.

Roshchina, V. V. (2012). Vital autofluorescence: Application to the study of plant living cells. *Journal of Biomedicine and Biotechnology*, *2012*(1), 1–14. http://dx.doi.org/10.1007/978-3-540-95894-9_8.

Shaner, N. C., Campbell, R. E., Steinbach, P. A., Giepmans, B. N. G., Palmer, A. E., & Tsien, R. Y. (2004). Improved monomeric red, orange and yellow fluorescent proteins derived from Discosoma sp. red fluorescent protein. *Nature Biotechnology*, *22*(12), 1567–1572. http://dx.doi.org/10.1038/nbt1037.

Shaner, N. C., Lambert, G. G., Chammas, A., Ni, Y., Cranfill, P. J., Baird, M. A., et al. (2013). A bright monomeric green fluorescent protein derived from Branchiostoma lanceolatum. *Nature Methods*. http://dx.doi.org/10.1038/nmeth.2413.

Shaner, N. C., Lin, M. Z., Mckeown, M. R., Steinbach, P. A., Hazelwood, K. L., Davidson, M. W., et al. (2008). Improving the photostability of bright monomeric orange and red fluorescent proteins. *Nature Methods*, *5*(6), 545–551. http://dx.doi.org/10.1038/nmeth.1209.

Shaner, N. C., Patterson, G. H., & Davidson, M. W. (2007). Advances in fluorescent protein technology. *Journal of Cell Science*, *120*(Pt 24), 4247–4260. http://dx.doi.org/10.1242/jcs.005801.

Shaner, N. C., Steinbach, P. A., & Tsien, R. Y. (2005). A guide to choosing fluorescent proteins. *Nature Methods*, *2*(12), 905–909. http://dx.doi.org/10.1038/nmeth819.

Shcherbo, D., Murphy, C. S., Ermakova, G. V., Solovieva, E. A., Chepurnykh, T. V., Shcheglov, A. S., et al. (2009). Far-red fluorescent tags for protein imaging in living tissues. *Biochemical Journal*, *418*(3), 567–574. http://dx.doi.org/10.1042/BJ20081949.

Shu, X., Shaner, N. C., Yarbrough, C. A., Tsien, R. Y., & Remington, S. J. (2006). Novel chromophores and buried charges control color in mFruits. *Biochemistry*, *45*(32), 9639–9647. http://dx.doi.org/10.1021/bi060773l.

Sinnecker, D., Voigt, P., Hellwig, N., & Schaefer, M. (2005). Reversible photobleaching of enhanced green fluorescent proteins. *Biochemistry*, *44*(18), 7085–7094. http://dx.doi.org/10.1021/bi047881x.

Tsien, R. Y. (1998). The green fluorescent protein. *Annual Review of Biochemistry*, *67*, 509–544. http://dx.doi.org/10.1146/annurev.biochem.67.1.509.

Wachter, R. M., Watkins, J. L., & Kim, H. (2010). Mechanistic diversity of red fluorescence acquisition by GFP-like proteins. *Biochemistry*, *49*(35), 7417–7427. http://dx.doi.org/10.1021/bi100901h.

Yarbrough, D., Wachter, R. M., Kallio, K., Matz, M. V., & Remington, S. J. (2001). Refined crystal structure of DsRed, a red fluorescent protein from coral, at 2.0-A resolution. *Proceedings of the National Academy of Sciences of the United States of America*, *98*(2), 462–467. http://dx.doi.org/10.1073/pnas.98.2.462.

Zacharias, D. A., Violin, J. D., Newton, A. C., & Tsien, R. Y. (2002). Partitioning of lipid-modified monomeric GFPs into membrane microdomains of live cells. *Science*, *296*(5569), 913–916. http://dx.doi.org/10.1126/science.1068539.